

A Three-Phase Step-Up DC-DC Converter with a Three-Phase High Frequency Transformer

S.V.G. Oliveira*, and I. Barbi**

*Regional University of Blumenau – FURB

Department of Electrical Engineering and Telecommunications – DEET – Blumenau, Brasil

**Power Electronics Institute - INEP

Federal University of Santa Catarina - UFSC

Department of Electrical Engineering - DEE, Florianópolis, Brasil

sergio_vidal@ieee.org - ivobarbi@inep.ufsc.br

Abstract — This paper presents a new 3-phase step-up DC-DC converter with a 3-phase high frequency isolation transformer. This converter was developed for industrial applications where the dc input voltage is lower than the output voltage, for instance in, installations fed by battery units, photovoltaic arrays or fuel cell systems. The converter's main characteristics are: reduced input ripple current, step-up voltage, high frequency isolating transformer, reduced output voltage ripple due to three pulsed output current and the presence of only three active switches connected at the same reference, this being a main advantage of this converter. By means of a specific switch modulation, the converter allows two operational regions. Theoretical expressions and experimental results are presented for a 6.8 kW prototype, operating in region R2 and for a 3.4 kW prototype operating in region R3, both in continuous conduction mode.

I. INTRODUCTION

The great necessity in several areas, especially the industrial sector, for switch mode power converters with larger power ratings at the end of the 80's was the starting point for the appearance of the high frequency three-phase dc-dc converter.

Since the first three-phase dc-dc isolated converter introduced by PRAZAD et al. 1988 [1], up until today, three-phase dc-dc development follows two paths, both with the same goal: to increase the electronic power density ratings. The new topologies are of the first path and have important propositions [1], [4], [6]. The second path is the soft commutation with its main contributions [2], [3], [5].

The typical architecture of a high frequency three-phase dc-dc isolated converter is depicted in Figure 1. In the input stage, the mostly common configuration is the stage operates like a voltage source, while the output stage has current source characteristics, [1], [2], [3], [5], [6]. The advantages of three-phase dc-dc isolated solutions are:

- ☞ Reduction of the input and output filters' volume; as well as, reduction of weight and size of the isolation transformers;

- ☞ Lower rms current levels through the power components, when compared to single phase solutions for the same power ratings. On the other hand, employing three-phase solutions increases circuits' complexity and the number of components. These characteristics can reduce application reliability.

The three-phase step-up dc-dc isolated converter presented in this article, Figure 2, has all of the main advantages of the three-phase solutions presented up until today. Moreover, the reduced number of switches plus the voltage step-up characteristic improves efficiency and reduces, along with a high switching frequency, the output filter volume, respectively. Furthermore, due to the input current source and step up voltage characteristics, this topology can be adopted in all types of applications supplied by alternative energy sources, like battery or photovoltaic arrays and the more recent, fuel cell systems. Three converter operation regions are defined, each one depending on the number of switches in overlapping conditions, Table 1. Theoretical expressions and experimental results are presented for a 6.8 kW prototype, operating in region R2 and for a 3.4 kW prototype operating in region R3, both in continuous conduction mode.

II. THE PROPOSED CONVERTER AND PRINCIPLE OF OPERATION

A. Circuit Description

Figure 2 shows the power-stage of the proposed circuit. The left-side of the circuit (inverter) comprises three inductors and three switches connected to a DC link. The right-side of the circuit is a traditional three branch six diodes rectifier with a capacitive output filter. A High frequency three-phase transformer links the two sides. The snubber circuit [7], containing: D_{s1} , D_{s2} , D_{s3} , R_s and C_s is used to control the overvoltage voltage across the switches during its turn-off instants. The three-phase step-up DC-DC isolated converter characteristics are:

- ☞ the proposed three-phase inverter (left-side) circuit presents a low input ripple current, because it acts as non-pulsed current source, independent of both operation modes and regions of the converter;

- ☞ the output voltage ripple is reduced due to the three-pulse output current; consequently a small capacitance value is required;

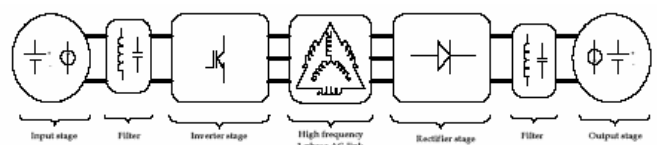


Figure 1 - Typical 3-phase DC-DC converter architecture.

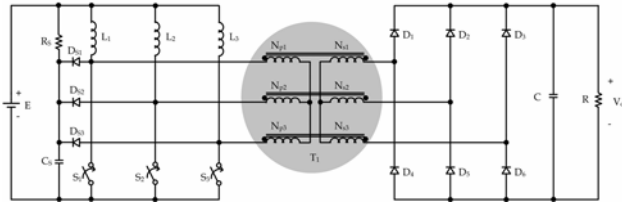


Figure 2– The three-phase step-up DC-DC isolated converter.

☞ only the three switches connected at the same reference, confers simplicity to the drive and control circuits;

☞ the voltage applied across the switches is reduced due to employed isolation transformer.

B. Analysis of operation

To facilitate the analysis of the circuit operation, Figure 3 shows a simplified circuit diagram. In the simplified circuit, T_{r1} is modeled as an ideal transformer with turns ratio $n=1$. Its is assumed that its magnetizing inductance is large enough that it can be neglected. Also, it is assumed that the filter capacitor C is large enough and, thus, its output voltage ripple is small compared to its DC voltage.

Finally, it is assumed that all semiconductor components are ideal, i.e., they present zero impedance when on and infinite impedance when off. The power flux transfer and the output/input voltage ratio are controlled by duty ratio D of the switches. A PWM technique is used for the switches S_1, S_2 e S_3 . The duty ratio D is defined by (1).

$$D = \frac{t_{ON}}{T_S} \quad (1)$$

Where, t_{ON} is the on time interval of the switches and T_S is the switching period.

C. Operation regions

The circuit proposed has three different operation regions according to the Table 1. Each one differs from other by the number of switches on at the same time (overlapping). For each region, the duty cycle ratio can assume different values. Due to the converter's input current source characteristics, at least one switch must always be on. Hence, the first region, R_1 , is forbidden. Figure 4 depicts a modulation of the switches for the converter's operation in region R_2 .

III. THEORETICAL ANALYSIS

A. Steady state stage operations for region R_2

Figure 3 shows four of the six topological stages of the converter's operation at R_2 region, during a switching period.

1) 1st stage (t_0, t_1) – Figure 7(a)

At the instant t_0 , switch S_1 is turned on and conducts along with switch S_3 . They are kept on during this stage. Inductances L_1 and L_3 store energy from source E . The energy stored in L_2 is transferred to the load through D_2, D_4 and D_6 . Currents $i_{D_4}(t)$ and $i_{D_6}(t)$ are, respectively, added to $i_{S_1}(t)$ and $i_{S_3}(t)$. This stage finishes at instant t_1 when S_3 is turned off.

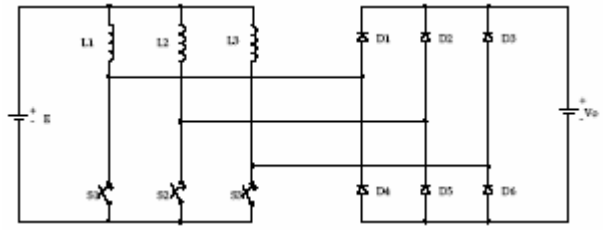


Figure 3– Simplified power-stage circuit diagram.

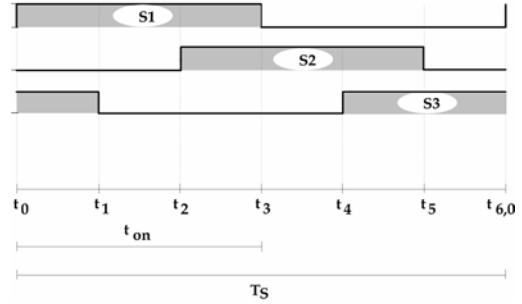


Figure 4 - Switches' modulation strategy for region R_2 .

TABLE 1-
OPERATION REGIONS FOR THE CONVERTER.

Regions	Duty cycle	Switches status
1	$D < 1/3$	Forbidden
2	$1/3 \leq D \leq 2/3$	Up to 2 overlapped
3	$D > 2/3$	Up to 3 overlapped

2) 2nd stage (t_1, t_2) Figure 7 (b)

At instant t_1 , S_3 is turned off and the energy stored in L_2 and L_3 is transferred to the load through D_3, D_2 and D_4 . Current $i_{D_4}(t)$ is added to $i_{S_1}(t)$. This stage finishes at instant t_2 when S_2 is turned on.

3) 3rd stage (t_2, t_3) Figure 7 (c)

At instant t_2 , S_2 is turned on. The energy of source E is stored in inductances L_1 and L_2 . The energy stored in L_3 continues to be transferred to the load through D_3, D_4 and D_5 . This stage finishes at instant t_3 when S_1 is turned off.

4) 4th stage (t_3, t_4) Figure 7 (d)

When S_1 is turned off, the energy stored in L_1 and L_3 is transferred to the load through D_1, D_3 and D_5 . Current $i_{D_5}(t)$ is added to $i_{S_2}(t)$. This stage finishes at instant t_4 when S_3 is turned on again.

5) 5th stage (t_4, t_5) Figure 7 (e)

At instant t_4 , the energy of source E is stored in inductances L_2 and L_3 . The energy stored in L_1 continues to be transferred to the load through D_1, D_5 and D_6 . This stage finishes at instant t_5 when S_2 is turned off.

6) 6th stage (t_5, t_6) – Figure 7 (f)

The converter's last stage of operation, for a T_S switching period, starts at the instant t_5 when S_2 is turned off. The energy from source E stored in inductances L_2 and L_1 is then transferred to the load through diodes D_1, D_2 and D_6 . Diode current $i_{D_6}(t)$ is added to switch current $i_{S_3}(t)$. At the end of this stage a converter operation switching period is finished.

B. Steady state stage operations for region R_3

Figure 5 depicts a modulation of the switches for the converter's operation in region R_3 .

1) 1st stage (t_0, t_1) – Figure 8(a)

At instant t_0 , switch S_1 is turn on and conducts along with switches S_2 and S_3 . Inductances, L_1, L_2 and L_3 , stored energy from source E . This stage finishes at instant t_1 when S_2 is turned off.

2) 2nd stage (t_1, t_2) – Figure 8 (b)

At instant t_1 , S_2 is turned off the energy stored in L_2 is transferred to the load through diodes D_2, D_4 e D_6 . Currents $iD_4(t)$ and $iD_6(t)$ are adds to currents $iS_1(t)$ and $iS_3(t)$, respectively. This stage finishes at instant t_2 when S_2 is turned on.

3) 3rd stage (t_2, t_3) – Figure 8 (a)

At instant t_2 , S_2 is turned on and the first stage is repeated. With the energy of the source being stored at inductances L_1, L_2 and L_3 . This stage finishes at instant t_3 when S_3 is turned off.

4) 4th stage (t_3, t_4) – Figure 8 (c)

When S_3 is turned off, the energy stored in L_3 is transferred to the load through D_3, D_4 and D_5 . Currents $iD_4(t)$ and $iD_5(t)$ are added to switch currents $iS_1(t)$ and $iS_2(t)$, respectively. This stage finishes at instant t_4 when S_3 is turned on again.

5) 5th stage (t_4, t_5) – Figure 8 (a)

At instant t_4 , S_3 is turned on and the first stage is repeated, with the energy off the source being stored in inductances L_1, L_2 and L_3 . This stage finishes at instant t_5 when S_1 is turned off.

6) 6th stage (t_5, t_6) – Figure 8 (d)

The last stage of converter operation starts at instant t_5 , with S_1 turning off and the energy stored in inductance L_1 being transferred to the load through diodes D_1, D_5 and D_6 . Diode currents $iD_5(t)$ and $iD_6(t)$ are added to switch currents $iS_2(t)$ and $iS_3(t)$, respectively. At the end of this stage, one period of switching operation is concluded.

IV. OUTPUT CHARACTERISTIC

Figure 6 shows the three operation regions related to the output characteristic of the proposed converter. There, the two modes of conduction of the converter can be observed.

The output/input gain, q , for operation area R2 (vertical line pattern) in CCM mode is limited to a maximum of 3 times the transformer's turns ratio. Otherwise, in region R3 (horizontal line pattern) the minimum value of the output voltage in CCM mode is 3 times the transformer's turns ratio. Gain q being the ratio between the output and the input voltage, for all modes and regions of operation is described by (2). Where, \bar{I}_o is the normalized output current, given by (3).

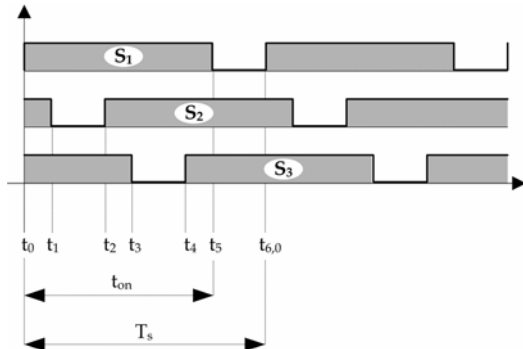


Figure 5 - Switches' modulation strategy for region R3.

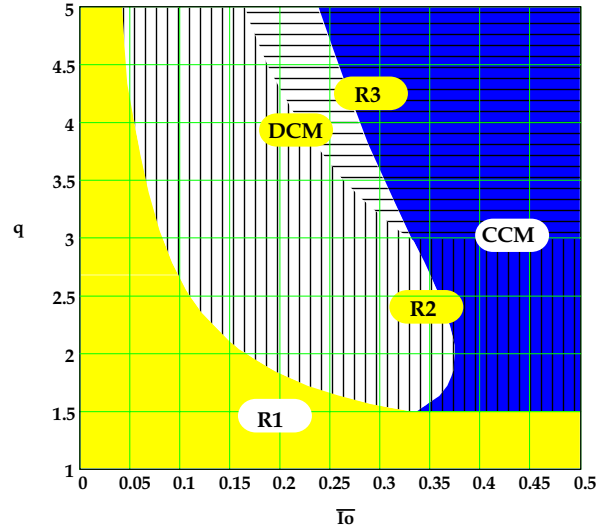


Figure 6 – Output characteristic of the proposed converter for a unity transformer turns ratio.

$$q = \frac{V_o}{E} = \begin{cases} q_{CCM} = n \left(\frac{1}{1-D} \right) \\ q_{CCM} = \frac{n}{4I_o} \left(3 \pm \sqrt{9 - 24\bar{I}_o} \right) \\ q_{DCM} = n + \frac{3}{2} \left(\frac{D^2}{\bar{I}_o} \right) \end{cases} \quad (2)$$

$$\bar{I}_o = \frac{I_o \cdot f_s \cdot L}{V_o} \quad (3)$$

V. DESIGN PROCEDURE

Below the main equations that can be used for determining of the input inductances and the exact expression for the output capacitor are described.

$$n = \frac{N_s}{N_p} \quad (4)$$

$$\bar{L}_C = L_C \cdot \frac{f_s \cdot I_o}{V_o} = \frac{3}{2} \left(\frac{q-n}{q^3} \right) \quad (5)$$

$$\Delta iE = \Delta iE \cdot \frac{f_s \cdot L}{V_o} = \frac{9n(q-n) - 2q^2}{3q^2} \quad (6)$$

$$C = \frac{I_o f_s L n q^2 [18n(q-n) - 4q] + V_o \{q^3 - n[7q^2 - 3n(5q-3n)]\}}{18q^3 n^2 f_s^2 L \Delta V_o} \quad (7)$$

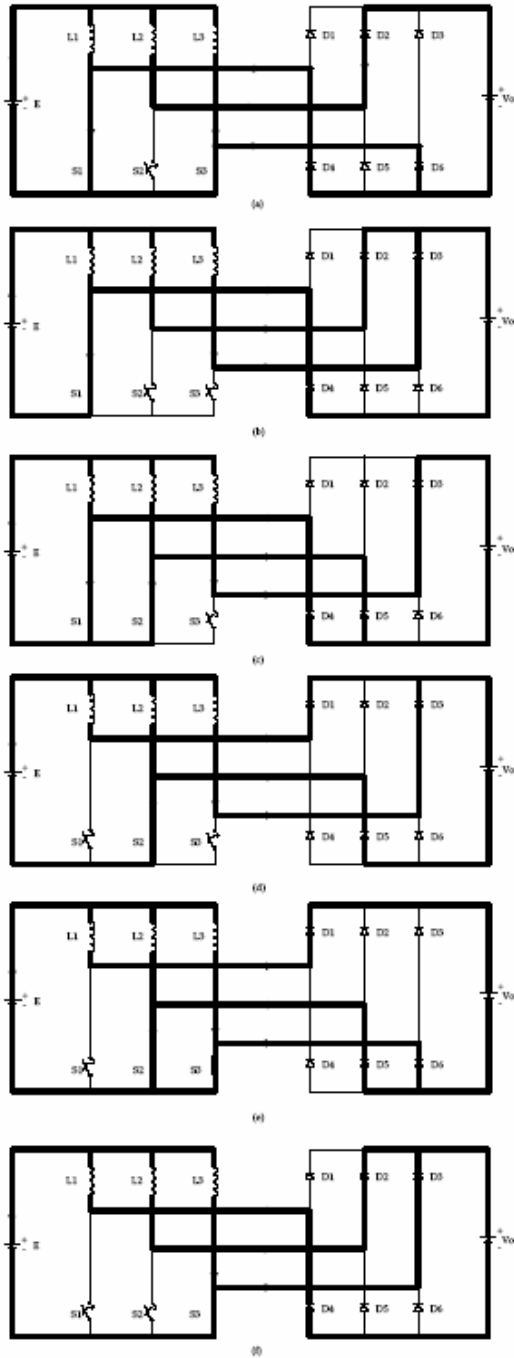


Figure 7 - Topological stages of the proposed converter in operational region R_2 .

VI. SIMPLIFIED DESIGN EXAMPLE

The goal of this analysis is to show the advantages of using the three-phase isolation transformer in a three-phase step-up dc-dc isolated converter. The experimental results are obtained for a system supplied by a 47V, 8kW DC link, in region R_2 . The system specifications are presented below.

- ☞ $P_o = 3.4\text{kW}$ and 6.8 kW , output power;
- ☞ $V_o = 450\text{ V}$, rated output voltage;
- ☞ $E = 27\text{Vdc}$ and 47 Vdc , rated input voltages;
- ☞ $f_s = 20\text{ kHz}$, switching frequency;

- ☞ $n=21/4$, transformer's turns-ratio;
- ☞ $\Delta V_o \leq 9\text{ V}$, output ripple voltage,
- ☞ $\Delta I_E \leq 3\text{ A}$, input ripple current.

A. Determination of the voltage gain

From the output and input rated voltages, gain q is given by (8).

$$q = \frac{450\text{V}}{47\text{V}} = 9.57 \quad (8)$$

B. Duty ratio

The duty cycle ratio is given by (9).

$$D = \frac{q - n}{q} = \frac{9.57 - 5.25}{9.57} \cong 0.45 \quad (9)$$

C. Determination of the input inductances

The value of the inductances were defined, taking into account that the converter keeps operating in the continuous conduction mode, even with 10% of the rated power. Under these conditions, the inductance values are given by (10).

$$L_{1,2,3} = \overline{I_C} \cdot \frac{10V_o}{f_s \cdot I_o} \cong 134\mu\text{H} \quad (10)$$

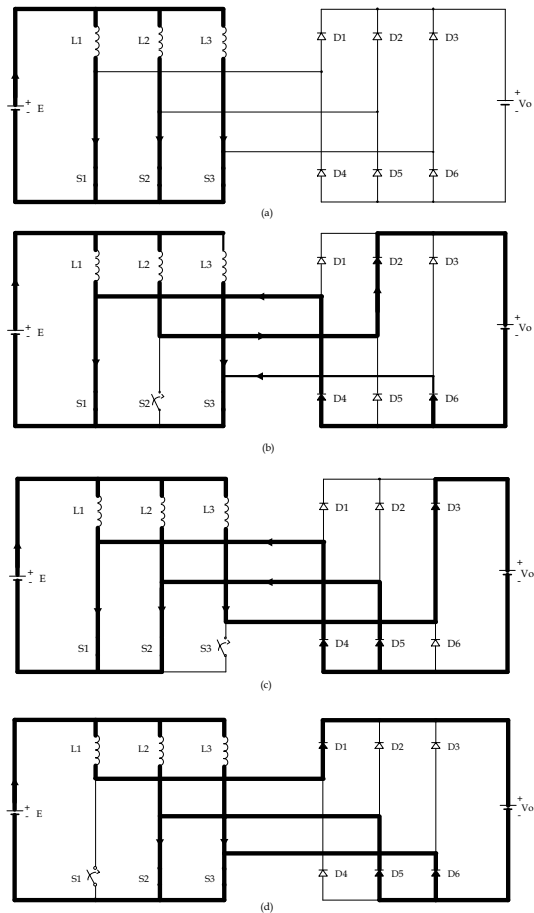


Figure 8 – Topological stages of the proposed converter in operational region R_3 .

D. Determination of the output capacitance

The exact value of output capacitance is obtained using (7). But, due to its *rms* current stress, it was changed to 2000 μ F/500V.

VII. PROTOTYPE DESCRIPTION

Using the design equations and for the converter specifications, a 6.8 kW prototype was implemented, Figure 9 The components employed were three 134 μ H inductor, built in a toroidal core of Kool μ [®] material; two output capacitors with 1000 μ F/500V (2XB43510) from Epcos[®]; three Mosfet switches SKM 121AR[®]. The output rectifier contains six diodes HFA15TB60 from IR[®]. The gate drive pulses are generated by a PIC[®] 16F873A μ controller. Employed three single-phase transformers in Y-Y connection, were operating as a three-phase high frequency transformer, with two ferrite cores 80-38-20 in parallel per phase of TSF 7070[®] material, see Figure 10. The inductor currents are measured by three *Hall* effect sensors, LA100P[®] from LEM[®]. Other details of the prototype, plus, experimental results for a 3.4 kW prototype operating in operational region R₃, will be presented in the final version of paper.

A. Experimental results

Figure 11, depicts the gate drive pulses of the switches. In Figure 12 shows the rated output voltage and the turn-off switches' voltages. From Figure 13 the three inductor currents of the *Hall* sensors plus the output voltage can be viewed. The currents through the inductors are obtained by the conversion: $i_L = 100 \cdot (v_{sensored} \div 13,5V) A$. The input current is the sum of the inductor currents. At Figure 14, are shows the commutation of the switch S₁, at the rated power of converter operation. The converter's efficiency is close to 88%. Figure 15, shows waveforms for a duty ratio of D=0.7, that is, the proposed convert is operating in operational region R3.

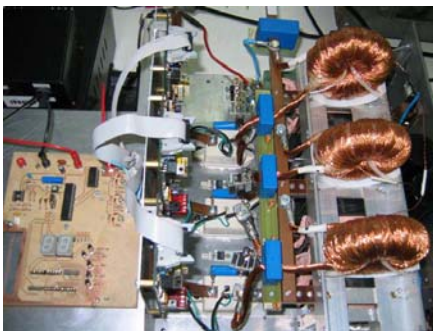


Figure 9 - Picture of the prototype.

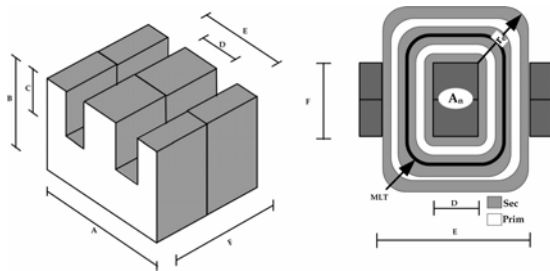


Figure 10 - Transformers' core configuration.

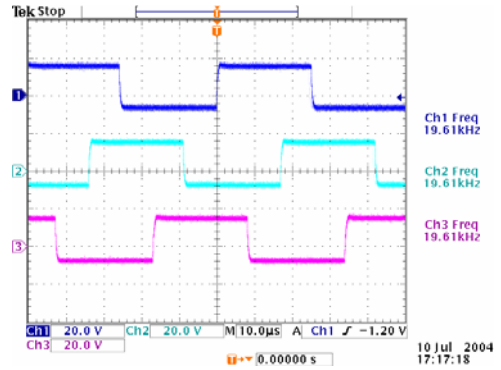


Figure 11 - Gate drive pulses.

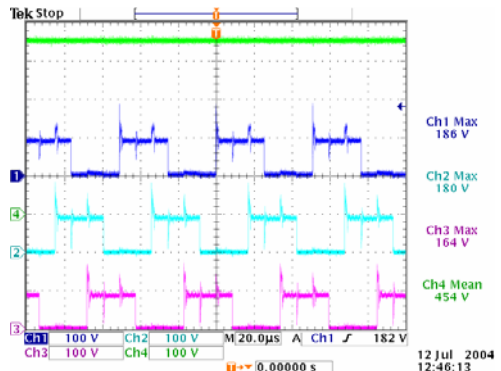


Figure 12 – Output voltage (Ch4) and switches' turn-off voltages.

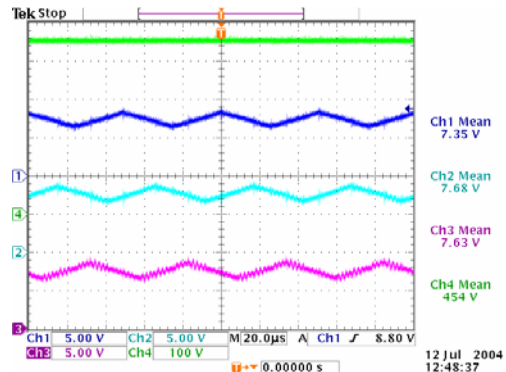


Figure 13 – Output voltage (Ch4) and inductor currents.

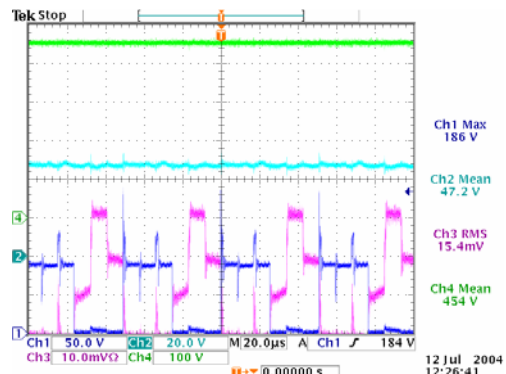


Figure 14 – Commutation of S₁, voltage (Ch1, with 50V/div) and current (Ch3 with 50A/div), plus, rated input and output voltages, Ch2 and Ch4, respectively.

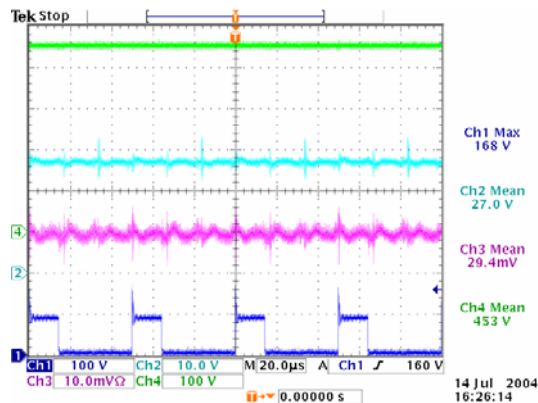


Figure 15 - Experimental results for operational region R_3 : Switch's turn-off voltage (Ch1), input current (Ch3-50A/div), rated input and output voltages, Ch2 and Ch4, respectively.

VIII. CONCLUSIONS

In order to develop a topology that presents greater efficiency with reduced weight and size, the three-phase step-up dc-dc isolated converter was presented. With these characteristics, this converter contains only three controlled switches and, a high frequency transformer. The input and output filters are fed by three times the switching frequency, which will reduce their volume. This converter can be used in all applications that require a reduced input ripple current e.g., in industrial applications, where the dc input voltage is lower than the output voltage, for instance in installations fed by battery units, photovoltaic arrays or fuel cell systems.

During its construction special care was taken in the constructing the transformer, mainly, with respect to the

reduction of its leakage inductance. This characteristic is an important constraint for choosing switching frequency.

The obtained efficiency, for the converter operating at region R_2 , close 88%, can be considered high, considering its rated power and that it works with hard-switching commutation.

With the goal of performing tests in both operational regions, using the same prototype, in region R_3 the results were obtained for a 3.4kW of output power, 27V of input voltage for the same rated output voltage.

REFERENCES

- [1] P. D. ZIOGAS, A. R. PRAZAD, S. MANIAS. Analysis and design of the three-phase off-line dc-dc converter with high frequency isolation. In: Proc IAS'88, pp. 813-820.
- [2] A. R. Prazad, P. D. Ziogas and S. Manias, "A three-phase resonant PWM dc-dc converter". In: 22nd Annual IEEE Power Electronics Specialists Conference, PESC '91 Record, p. 463-473, 1991.
- [3] D. S. Oliveira Jr. and I. Barbi, "A three-phase ZVS PWM dc-dc converter with asymmetrical duty-cycle for high power applications" In: 34th IEEE Power Electronics Specialists Conference, PESC'03 Record, p. 616-621, 2003.
- [4] R.W.A.A De Doncker, D. M. Divan, M. H. A. Kheraluwala, "Three-phase soft-switched high-power-density DC/DC converter for high-power applications". In: IEEE Transactions on Industry Applications, Vol.: 27 Issue: 1 Part: 1, p. 63-73, Jan.-Feb. 1991.
- [5] BHAT, A. K. S; ZENG, L. Analysis and design of three-phase LCC-type resonant converter. In: IEEE Power Electronics Specialists Conference, PESC '96. Record, p. 252-258, 1996.
- [6] L. D. Salazar, P. D. Ziogas, "Design oriented analysis of two types of three-phase high frequency forward SMR topologies". In: Fifth Annual Applied Power Electronics Conference and Exposition, APEC '90, Conference Proceedings, p. 312-320. 11-16/Mar, 1990.
- [7] F. J. Nome and I. Barbi, "A ZVS clamping mode current-fed Push Pull DC-DC converter". In: IEEE International Symposium on Industrial Electronics ISIE'98, Jul/ 1998, pp. 617-621.